J Mater Sci (2009) 44:655–663
DOI 10.1007/s10853-008-3062-7

X-ray diffraction investigations of α-polyamide 6 films: orientation and structural changes upon uni- and biaxial drawing

H. Shanak · K.-H. Ehses · W. Götz · P. Leibenguth · R. Pelster

Received: 14 August 2008 / Accepted: 15 October 2008 / Published online: 10 November 2008

Abstract We have investigated the influence of drawing on orientation, crystallinity, and structural properties of polyamide 6 films using X-ray diffraction. The samples were uniaxially and biaxially stretched resulting in the formation of monoclinic crystallites (α-form) in the size range of 8–10 nm. Depending on the drawing ratio, a degree of crystallinity of up to 60% is obtained. The average orientation of the crystallite axes was evaluated using the pole figure technique. The b^*-axis, which corresponds to the chain direction of the polyamide molecules, lies in the film plane and shows a preferred orientation upon drawing. For uniaxial drawing, b^* aligns with the drawing direction. For biaxially drawn films, which were prepared using the sequential stretching method, the second drawing determines the orientation of b^*, at least at the center of the films. At the sides, b^* is located between the two drawing directions reflecting the inhomogeneous distribution of mechanical stress during stretching.

Introduction

Polyamide 6 has been widely investigated because of its potential for application in different fields of technology, especially as engineering plastics [1, 2]. For example, it is a component in blends to be used in packaging applications for foods serving as a diffusion barrier for oxygen. Polyamide 6 was produced commercially for a long time in the form of fibers and films. The different properties of this material were studied as a function of the production conditions. The crystal structure of polyamide 6 films and fibers has been investigated by various authors [3]. The literature concerning the quantitative analyses of polyamide 6 by wide angle X-ray diffraction is fragmented and often contradictory [4]. But little information is available about the structural change during stretching of polyamide 6 films [1]. Stretching is part of the standard procedure for the industrial production of polyamide 6, leading to an increase of crystallinity and mechanical stability. The resulting partial molecular orientation reflects in the anisotropy of material parameters, e.g., the refractive index [1]. In order to improve quality and homogeneity of films, it is important to quantitatively relate the microstructure of the semicrystalline polyamides to their production history by techniques such as X-ray diffraction analysis [4]. Previous studies [5, 6] showed that depending on the production conditions mainly two stable crystallographic forms exist, α and γ, both as monoclinic structures, where the molecules are oriented parallel or anti-parallel to the b-axis (see Fig. 1). In the α-form, hydrogen bonds connect the anti-parallel chains of polyamide 6 whereas in the γ-form these bonds connect the parallel chains. The unit cell parameters of the α-form are $a = 9.56$ A, $b = 17.24$ A, $c = 8.04$ A, and $\beta = 67.5°$, and the parameters of the γ-form are $a = 9.33$ A, $b = 16.88$ A, $c = 4.78$ A, and $\beta = 121°$ [3, 6]. In some cases, the γ-form was indexed as pseudohexagonal [7, 8].

In this study, the effect of uniaxial and biaxial drawing on the structure formation of polyamide 6 films will be

H. Shanak · K.-H. Ehses · R. Pelster (✉)
Experimentalphysik, FB7.2, Universität des Saarlandes, 66123 Saarbrücken, Germany
e-mail: rolf.pelster@mx.uni-saarland.de

W. Götz
BASF SE Company, 67056 Ludwigshafen, Germany

P. Leibenguth
Werkstoffwissenschaften, Universität des Saarlandes, 66123 Saarbrücken, Germany

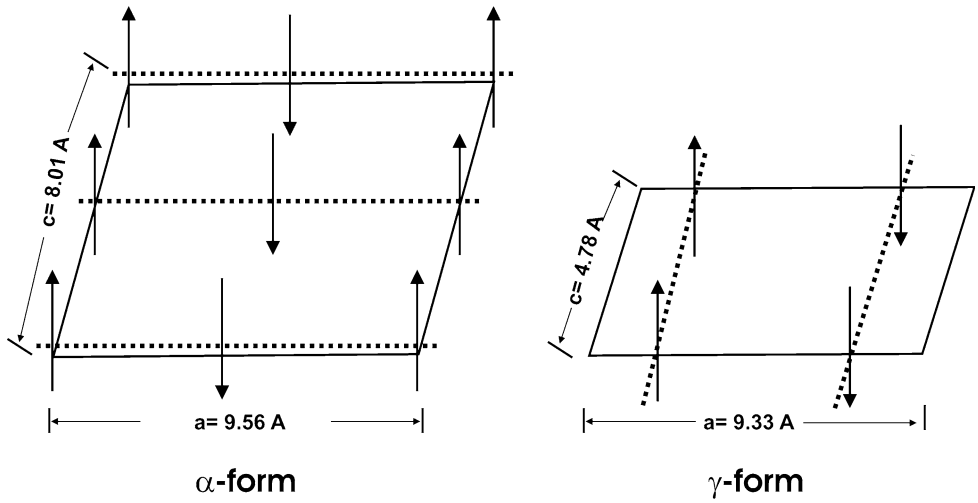

Fig. 1 A representation for the α- and the γ-form of polyamide 6 according to [3]. The dotted lines indicate the direction of hydrogen bonds; the arrows indicate the parallel and the anti-parallel chains

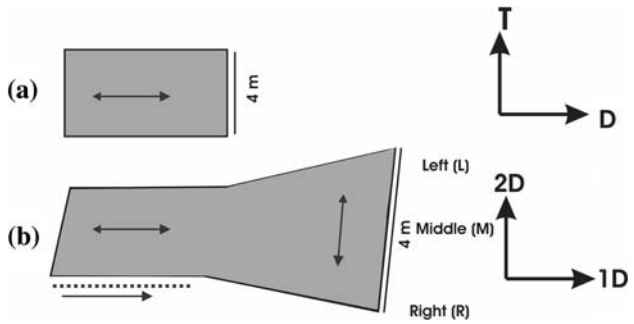

Fig. 2 A schematic representation of **a** the uniaxial and **b** the biaxial drawing of polyamide 6 films. In **a** D denotes the drawing direction and T the transverse direction. In **b** 1D is the first drawing direction (corresponding to the machine direction) and 2D the second drawing direction

analyzed mainly by X-ray diffraction (XRD). The microstructure, the degree of crystallinity, and above all the average orientation of the crystallites will be the subject of discussion in this paper. The latter aspect will be discussed in terms of the pole figure technique [9]. We are particularly interested in the homogeneity of the stretching process, i.e., we want to find out to which extent the orientation varies across the film width in commercially produced biaxially stretched films (see Fig. 2b).

Experimental

The investigated polyamide 6 films were produced by BASF Company from commercially available polyamide (UltramidR B33L) on a Barmag cast film line at 20 °C chill roll temperature. Monoaxially oriented film was made from this utilizing a laboratory stretching unit of Brueckner GmbH, Siegsdorf/Germany. The film samples of 150 μm thickness (made as mentioned above) were preheated to 190 °C and then stretched at drawing ratios from 1:2.0 to 1:4.0 (see Fig. 2a). Further, biaxially oriented (by sequential stretching method) film of MF Feinfolien GmbH, Kempten/Germany, was used (see Fig. 2b). This film was manufactured by extruding a 135 μm cast film to a chill roll of 16 °C, heating it up to 68 °C followed by drawing in the machine direction at a ratio of 1:2.8 (first drawing direction, 1D, see Fig. 2b). The film was then heated further to 85 °C and drawn by tenter frame in transverse direction (perpendicular to machine direction, which is called the second drawing direction, 2D, Fig. 2b) with a draw ratio of 1:3.3. Finally the film was heat-set at 205 °C and then cooled to 25 °C. The biaxial drawn films were investigated on different positions, i.e., on the left side, on the middle and on the right side of the film (see Fig. 2b).

In order to determine the crystal structure, degree of crystallinity, and size of crystallites, we have carried out XRD measurements with a Bragg-Brentano geometry. The measurements were performed in reflection and in transmission using Cu Kα and Mo Kα radiation, respectively. The angular resolution was 0.02°, the measuring time per step 20 s. Two techniques were employed to study the orientation of the crystallites: two-dimensional X-ray photographs were produced by the use of Ni-filtered Cu Kα radiation in the transmission mode (wide angle X-ray scattering, WAXS); in addition, pole figure data was obtained with an automated X-ray diffractometer (Panalytical X'Pert MRD System), using the geometrical configuration of Decker, Asp and Harker [10] with Nickel-filtered Cu Kα radiation. The Bragg angle 2θ was set at a particular (hkl) diffraction peak, and the sample was tilted by angle Φ and rotated by angle Ψ as shown in Fig. 3a [9]. In this case, the intensity I(Φ, Ψ) was measured as a function of Ψ for different steps of Φ, while Φ was held constant during each Ψ scan. The range of measurement for Φ was between 0° and 90°, with steps of 5°, and the range of Ψ was between 0° and 360°, with steps of 5°.

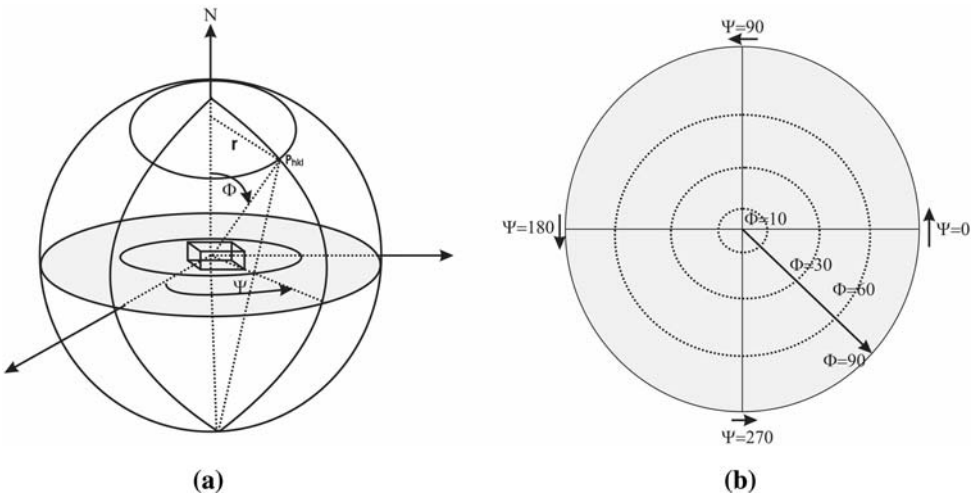

Fig. 3 **a** Geometry for the pole figure measurements: position of plane normal P_{hkl} specified by spherical coordinates Φ and Ψ. Φ is the angle between the sample axis N (the film normal) and the reciprocal lattice vector P_{hkl}. **b** A schematic representation showing the angles Φ and Ψ in a pole figure

Results and discussions

Crystal structure, degree of crystallinity and size of crystallites

Figure 4 presents the XRD patterns of undrawn and uniaxially drawn films of polyamide 6. The diffractogram of the unstretched film shows an amorphous structure. The XRD patterns of all uniaxially drawn films (drawing ratios 1:2, 1:3, and 1:4) show reflections that are characteristic for the monoclinic α-form. The intensity of some peaks increases with increasing drawing ratio. This shows the influence of stretching on the different properties of the film such as the orientation and the degree of crystallinity (see below).

In Fig. 5 we show the XRD patterns of a biaxially stretched film of polyamide 6 (sequential drawing, see Fig. 2b). The investigated parts of the film were the left side (L), the middle (M), and the right (R) side (compare with Fig. 2b). The patterns of the film show a monoclinic structure of the α-form. The positions of all reflections are at the same diffraction angles (2θ) for the left, middle, and right sides of the investigated film. But the intensity of the peaks depends on the position (L, M, R). This is due to the difference in the local crystallization ratio and the local degree of orientation of the films (see below). Additional measurements that confirm the crystalline structure are described in the appendix.

The degree of crystallinity was calculated for the different films and is shown in Fig. 6 (for the method, refer to Refs. [11, 12]). For the uniaxially drawn films, it increases from 28% at a drawing ratio of 1:2 to about 50% at a drawing ratio of 1:4. It is higher for the biaxially drawn films, where its value is about 60%. From the XRD patterns, the respective grain sizes were calculated by the use of a Williamson–Hall–Plot based on an evaluation of peak widths [13]. The result is displayed in Fig. 7. The grain sizes are in the range of 8–10 nm.

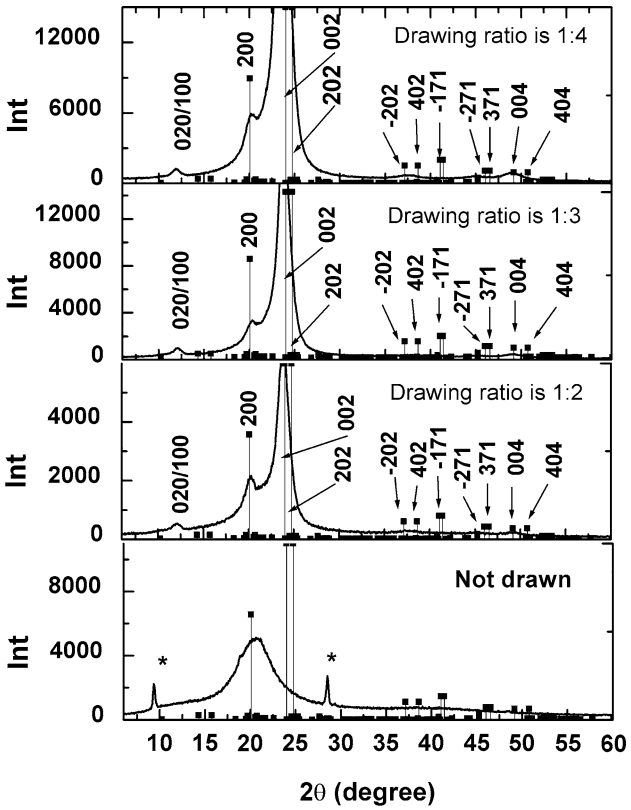

Fig. 4 XRD patterns of an undrawn and uniaxial drawn films of polyamide 6 (drawing ratios from 1:2 to 1:4). The undrawn film is amorphous (the peaks marked by an asterisk are caused by metal oxides). The stretched films show reflections that are characteristic for the monoclinic α-form: these are inter alia the 100/020 reflection at $2\theta = 11.77°$, the 200 reflection at $2\theta = 20.5°$, and the 004 reflection at $2\theta = 49.1°$. The strong reflection between $2\theta = 22.5°$ and 25° is caused by an overlap of 002 and 202 reflections

Orientation of the crystallites

First we performed transmission measurements (WAXS) in order to show qualitatively the effect of stretching.

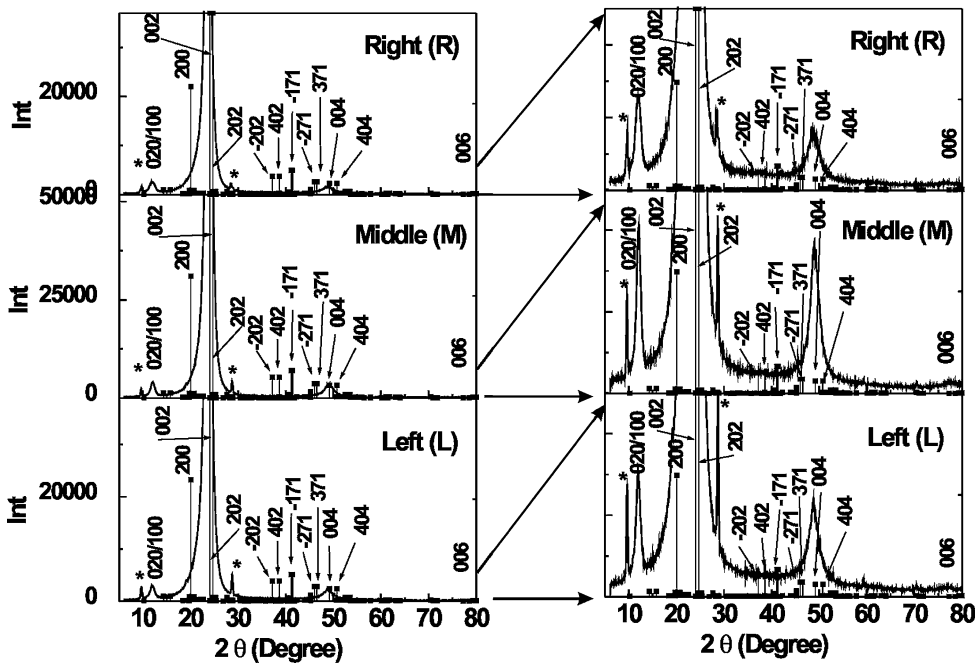

Fig. 5 XRD patterns of biaxial drawn polyamide 6 film investigated on the left side (L), in the middle (M), and on the right (R) side of the films (see Fig. 2b). The figures on the right hand show the same data but with an enlarged y scale. The peaks were indexed with a monoclinic α-form (peaks marked by an asterisk are caused by metal oxides). The 020/100 reflection is located at $2\theta = 11.9°$, the intensities of 200, 002, and 202 reflections overlap between $2\theta = 20°$ and 25°, where 200 is located at $2\theta = 20.08°$, 002 at $2\theta = 24.02°$, and 202 at $2\theta = 24.75°$. The 004 reflection is located at $2\theta = 49.18°$

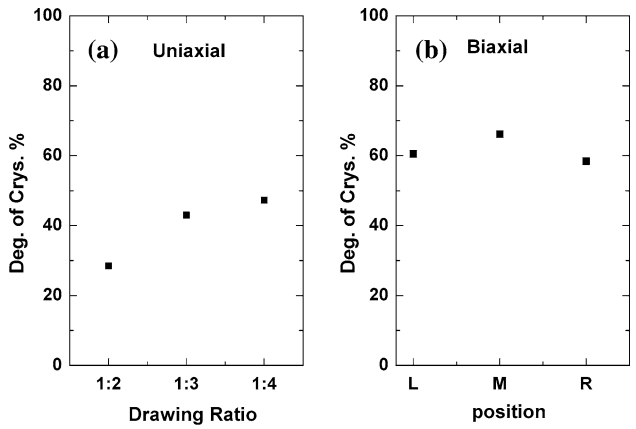

Fig. 6 The degree of crystallinity as a function of the drawing ratio (1:2, 1:3, and 1:4) for uniaxially drawn films (**a**) and as a function of position for biaxially drawn films (**b**) (L: left, M: middle, and R: right; see Fig. 2b)

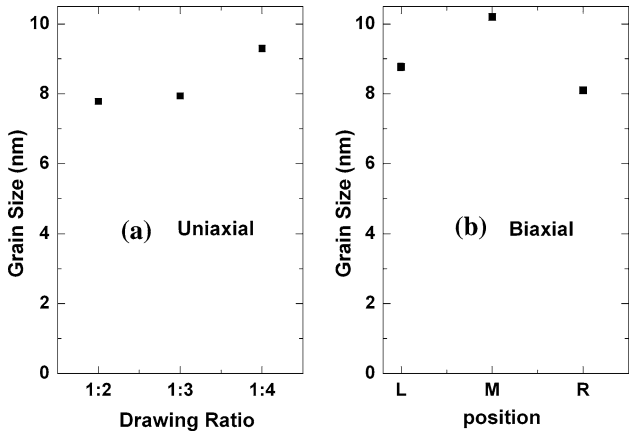

Fig. 7 The grain size as a function of the drawing ratio (1:2, 1:3, and 1:4) for uniaxially drawn films (**a**) and as a function of position for biaxially drawn films (**b**) (L: left, M: middle, and R: right; see Fig. 2b)

Figure 8a–d displays X-ray photographs of different polyamide films. The photograph of the undrawn film, Fig. 8a, shows that it is isotropic and not oriented. The patterns for the uniaxially stretched films (Fig. 8b–d) reflect the formation of a symmetry axis along and perpendicular to the drawing direction. The film of low elongation (drawing ratio of 1:2; see Fig. 8b) shows two rings. The inner one represents the 200 reflection [14]. It exhibits a nearly homogenous intensity with a weak increase at different positions. The outer ring represents the 002 reflection. Its intensity is high at the equator and decreases to a very low value on the meridian. At a drawing ratio of 1:3 (Fig. 8c) only two pairs of arcs are visible having a higher intensity in the equator. These become even smaller and more intense for the highest elongation of 1:4 (Fig. 8d). Summarizing, stretching causes both a higher degree of crystallinity (Fig. 6a) and a stronger orientation.

The Fig. 9a–c shows X-ray photographs of biaxially drawn films investigated at different positions, i.e., at the center and at the sides (see Fig. 2b). As before, each photograph shows two small concentric rings that are characteristic of the 200 and 002 reflections. The 200 ring reflects a preferred orientation of crystallites that depends on the position on the film. Figure 9a, the X-ray photograph of the left part of the film, shows two arcs with higher intensity in the first and the third quarter of the X-ray photograph. For the right part of the film (Fig. 9c), these arcs lie in the second and the fourth

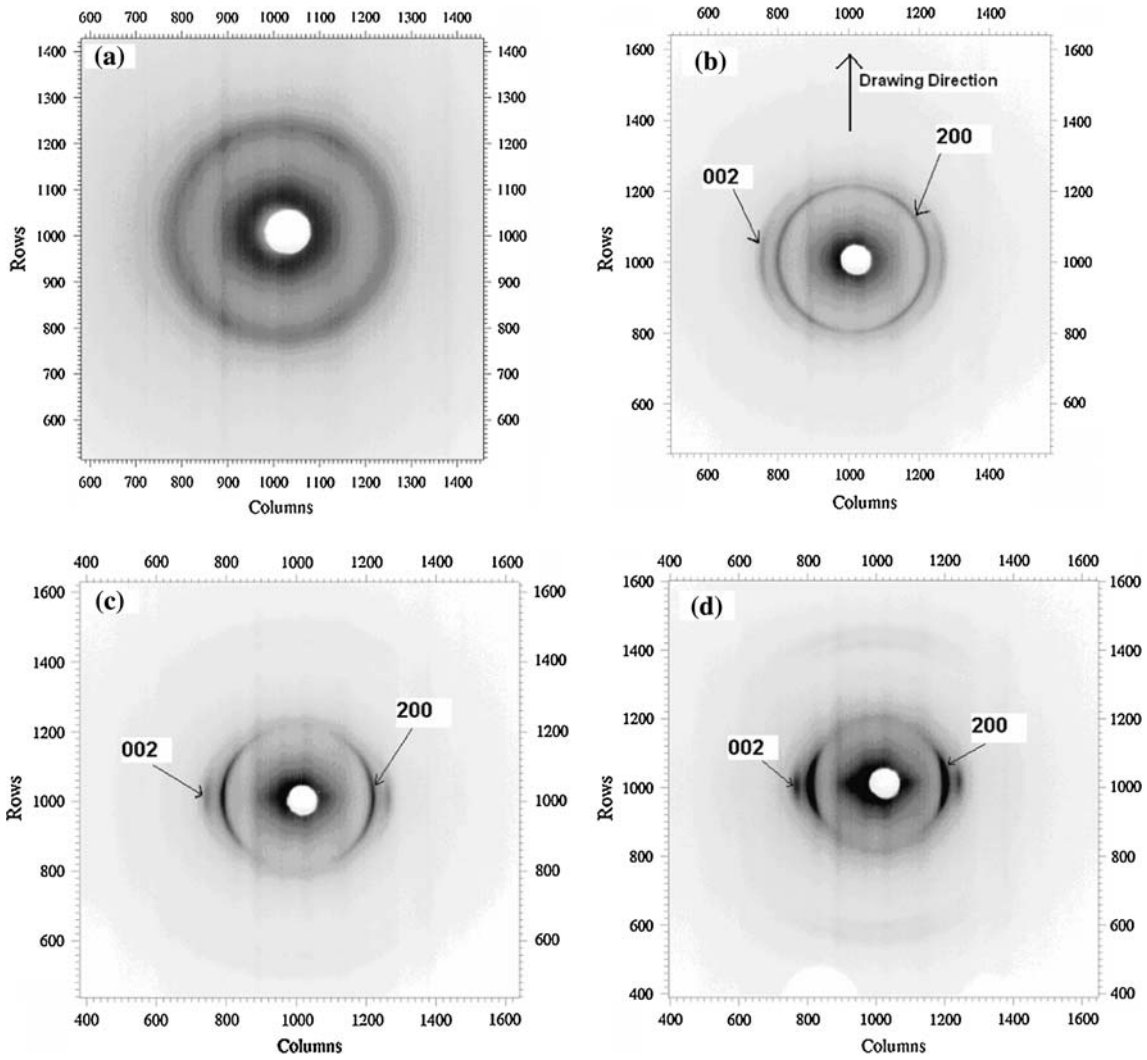

Fig. 8 **a–d** X-ray photographs of transmission measurements on polyamide 6 films for undrawn (**a**) and uniaxially drawn films with drawing ratio 1:2 (**b**), 1:3 (**c**), and 1:4 (**d**)

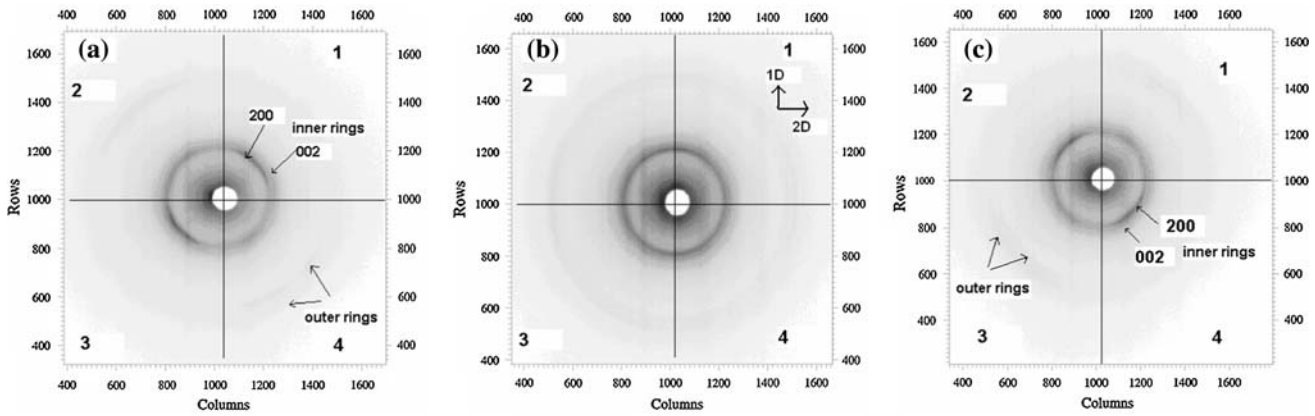

Fig. 9 **a–c** X-ray photographs of transmission measurements on a biaxially drawn polyamide 6 film on the left side (**a**), the middle (**b**), and the right side (**c**). (positions L, M, R; see Fig. 2b). 1D and 2D are the first and the second drawing direction, respectively

quarter. This mirror symmetry along the 1D direction (machine direction) reflects the symmetric production conditions sketched in Fig. 2b. For the middle part of the film, the intensity of the 200 reflection is distributed more homogeneously (Fig. 9b), indicating a more random crystal orientation compared to that at the sides.

In the next step we wanted to analyze in detail the influence of stretching on the average orientation of the crystallites. For such a quantitative analysis we used the X-ray pole figure technique (see Fig. 3). In the case of uniaxially stretched films with different ratios (1:2, 1:3, and 1:4; see Fig. 10), the pole figures of the 002 reflection show that the reciprocal c*-axis is strongly oriented in the direction of the normal to the film surface (maximum intensity at $\Phi = \Psi = 0°$, compare with Fig. 3). The pole figure of the 200 reflection for the film of low elongation with a drawing ratio of 1:2 shows that the reciprocal a*-axis is randomly distributed. The pole figures of the 200 reflection for the films of higher elongations with a drawing ratios of 1:3 and 1:4 show two peaks with maximum intensity at $\Phi = 66°$ and $\Psi = +90°$ or $\Psi = -90°$. These Ψ values show that the reciprocal a*-axis is strongly oriented transverse to the stretching direction. The value of Φ indicates an angle of about 66° between the a*-axis and

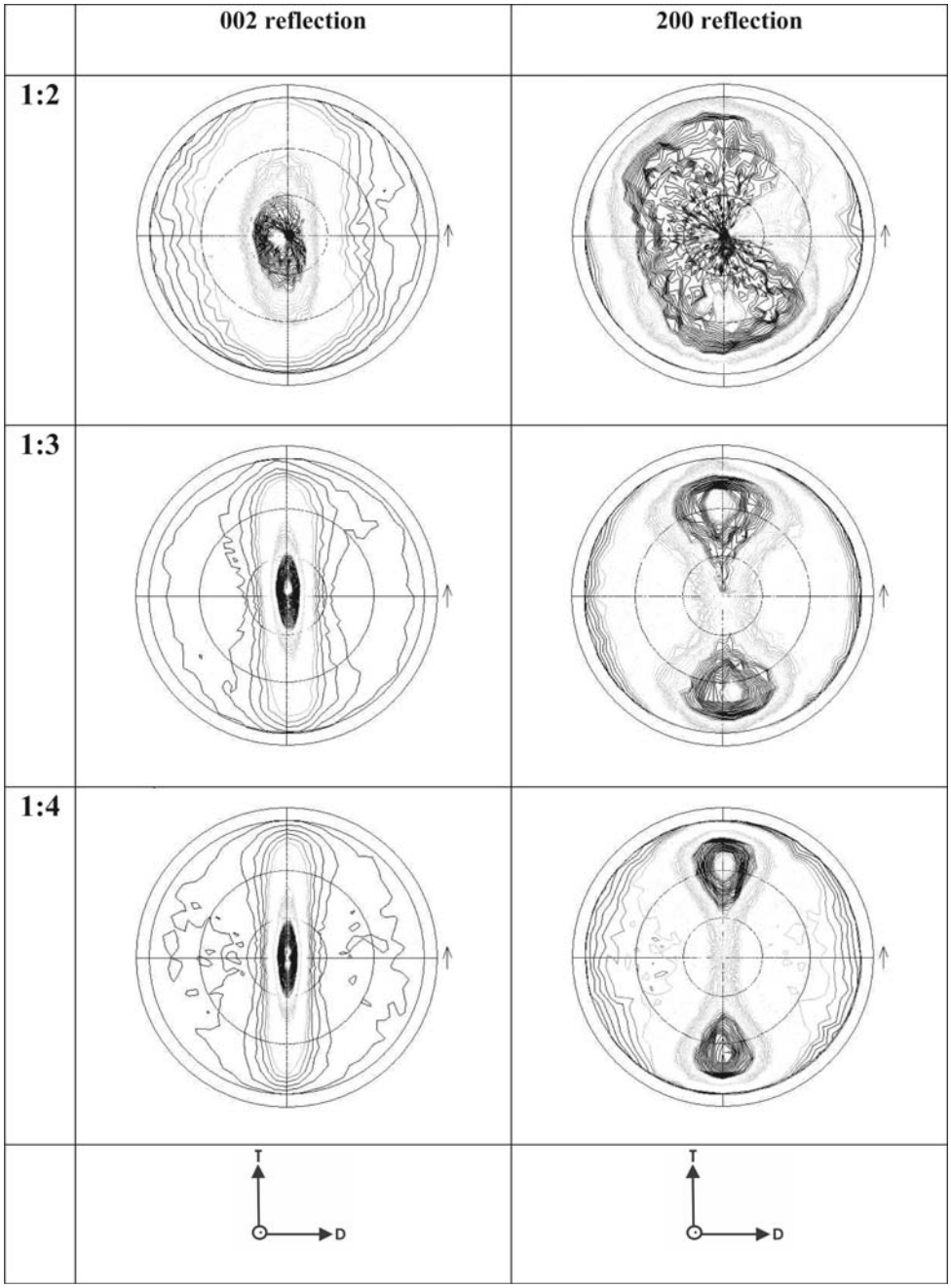

Fig. 10 Pole figures of the 002 and 200 reflections for polyamide 6 films drawn uniaxially with different ratios (1:2, 1:3 and 1:4). For the coordinates we refer to Fig. 3b

the normal (c*-axis). This is consistent with the geometry of the monoclinic α-form. According to this model, the b*-axis is perpendicular to the a*c*-plane, and it is located in the plane of the film and in the drawing direction. This means that the crystallographic axis a is in the transverse direction, the axis b or b* is in the drawing direction, and the axis c* is in the normal direction. Figure 11 shows the location of the different crystallographic axes with respect to the film axes, the stretching, and the transverse direction. One should remember that the molecules forming the crystallites are oriented parallel or anti-parallel to the b- or b*-axis (Fig. 1a). Thus stretching causes an average orientation of the molecule axes parallel to the drawing direction.

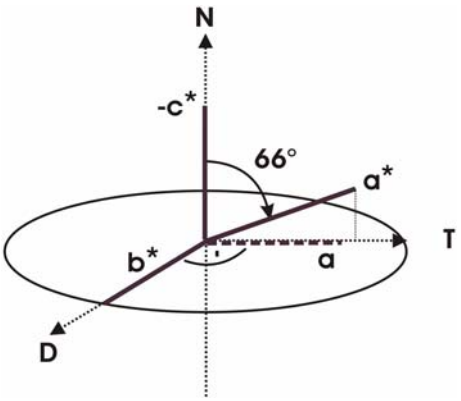

Fig. 11 A sketch illustrating the average orientation of crystallites in uniaxially drawn films: the location of the a-, a*-, b*- and c*-axis with respect to the drawing and transverse directions is shown (N is the normal to the surface of the film)

Now let us see how biaxially stretched films behave. The pole figures of the 002 reflection in Fig. 12 show that the c*-axis is always oriented in the direction of the normal to the surface of the film (maximum intensity at $\Phi = \Psi = 0°$, compare with Fig. 3). But the pole figures of the 200 reflection indicate that the orientation of the a*-axis depends on the position on the film. At the center of the film (M), the a*-axis is oriented in the first stretching direction (maximum at $\Psi = 0°$ or $\Psi = 180°$) transverse to the second drawing direction. The maximum intensity at $\Phi = 66°$ shows that the a*-axis makes an angle of 66° with the normal of the film surface, in addition to a mild random orientation. On the left side of the film (L) the a*-axis is located between the two drawing directions (maxima at $\Psi \approx +131°$ or $\Psi \approx -41°$) while it keeps the same angle of 66° with the normal to the film surface. On the right side of the film, the opposite orientation is observed ($\Psi \approx +40°$ or $\Psi \approx -130°$; compared to the left side this is a mirror symmetry with respect to the 1D or 2D axis). Figure 13 presents the location of the crystallographic reciprocal axes (a*, b*, and c*) with respect to both drawing directions. The orientation is not homogeneous across the film width but symmetric with respect to the machine direction (1D, see Fig. 2b). As already mentioned, the molecules are aligned parallel or anti-parallel to the b (or b*)-axis (see Fig. 1a). Thus, at the center of the film their orientation coincides with second drawing direction, i.e., it is perpendicular to the machine direction (see Fig. 2b).

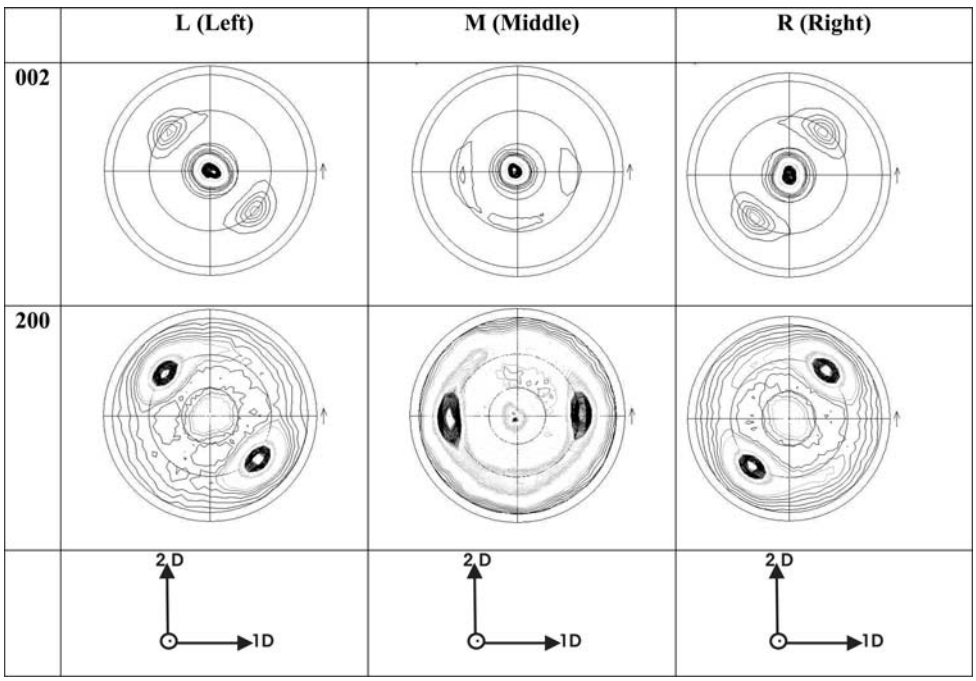

Fig. 12 Pole figures of the 002 and 200 reflections for a biaxially drawn polyamide 6 films. The film was investigated on the left (L), on the middle (M), and on the right (R) side (see Fig. 2b). For the coordinates we refer to Fig. 3b

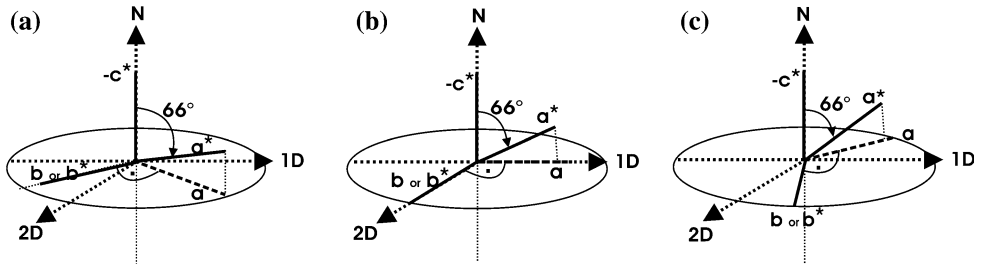

Fig. 13 A sketch illustrating the average orientation of crystallites in biaxially drawn films: the location of the a^*-, b^*-, and c^*-axis with respect to the first and to the second drawing direction is shown for positions on the left side (**a**), in the middle (**b**), and on the right side (**c**) of the film (see Fig. 2b)

Conclusions

Uni- and biaxial drawing influences the properties of polyamide 6 films. We have observed the formation of crystallites with a monoclinic α-form and with grain sizes of about 8 nm that orient themselves upon drawing.

For uniaxial drawing, the degree of crystallinity is directly proportional to the drawing ratio. The reciprocal c^*-axis is strongly oriented in the normal direction of the film. The b^*-axis lies in the surface of the film. With increasing drawing ratio a preferred orientation is observed: on average, b^* becomes orientated parallel to the drawing direction.

For biaxially drawn films, even higher crystallinities of about 60% are obtained, the exact values depending on the position on the film. As in the uniaxial case, the reciprocal c^*-axis is always strongly oriented in the normal direction of the film. The orientation of the b^*-axis is strongly affected by the drawing. In the middle of the film, the b^*-axis is oriented in the second drawing direction, i.e., transverse to the machine direction. At the sides of the film, it is located between the two drawing directions.

The observed orientation of the b^*-axis upon drawing coincides with that of the long polyamide molecules in the crystallites. In the monoclinic α-form of polyamide 6, the molecules are arranged parallel or anti-parallel to the b^*-axis. Therefore, we can interpret the above results in terms of molecular orientation. Upon drawing, the long molecules align with the direction of the local stress. For uniaxial stretching this is the drawing direction. For biaxial stretching the second drawing direction determines the final orientation, at least in the middle of the film. At the sides, systematic local distortions, i.e., an average orientation between both drawing directions, are observed.

Appendix

Some sample rotations were done during the measurement of the X-ray diffractograms in order to be sure about indexing the film reflections, to detect more peaks, and to

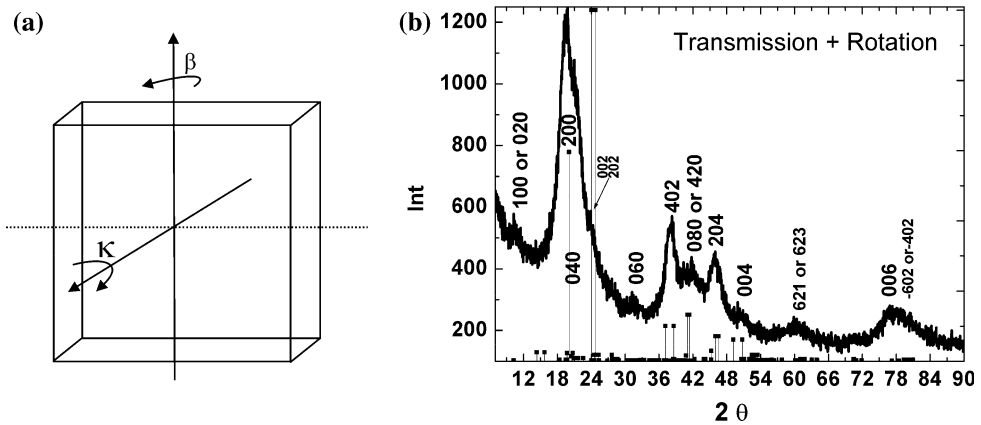

Fig. 14 **a** A schematic representation of the rotation angles β and κ. **b** Transmission intensity of XRD patterns of a biaxially drawn Polyamide 6 film, taken at its left side (L; see Fig. 2b). The film was continuously spun around the κ angle during the 2θ scan (In Figs. 14b, 15 and 16 data of Mo Kα radiation were converted into equivalent Cu Kα radiation for comparison)

separate the overlapping ones. In general, the rotations were done in κ and β angles as sketched in Fig. 14a. Figure 14b shows the transmission intensity of the XRD patterns of the biaxially drawn film taken from the left side (L; see Fig. 2b). The film was continuously spun in κ angle during the measurement. A comparison with Figs. 4 and 5 shows that new peaks appear.

Figure 15 presents the transmission XRD patterns of the same film, but now the angle β was fixed at +30, 0, and −30 degrees during the 2θ scan. At $\beta = -30°$, the peaks 200 at $2\theta = 20.5°$ and 002/202 at $2\theta = 24.05°$, which were previously overlapping (at $2\theta = 20°$–$25°$), can be separated. In Fig. 16, the angle κ was changed and β was kept constant at 30°. So it was possible to separate the 200 and 002 peaks, and to detect others such as the 006 peak, especially at $\beta = 30°$ and $\kappa = 45°$.

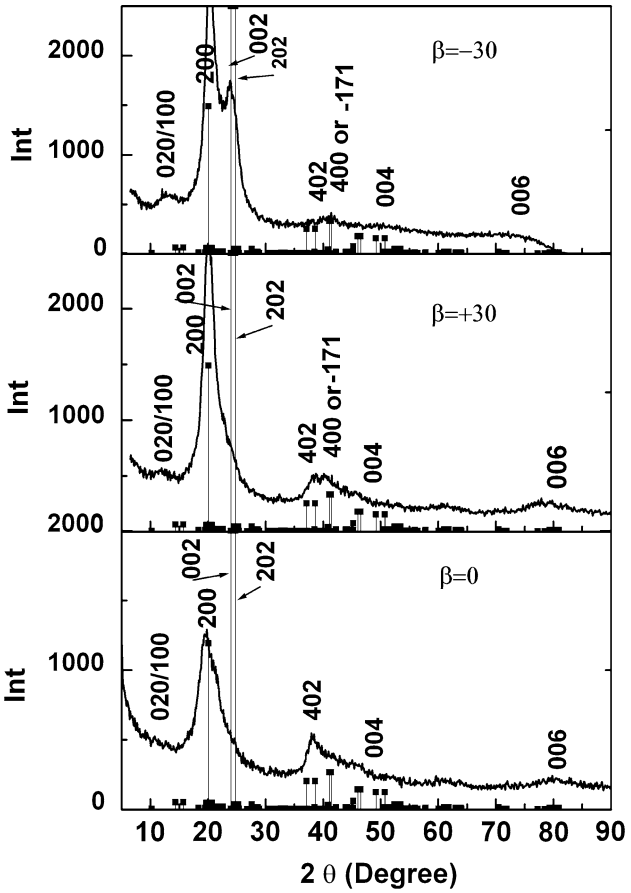

Fig. 15 Transmission intensity of XRD patterns (2θ-scan) for a biaxially drawn Polyamide 6 film, taken at its left side (L; see Fig. 2b). The film was oriented by the angle β ($\beta = -30°$, 0°, +30°) while the angle κ was kept constant (see Fig. 14a)

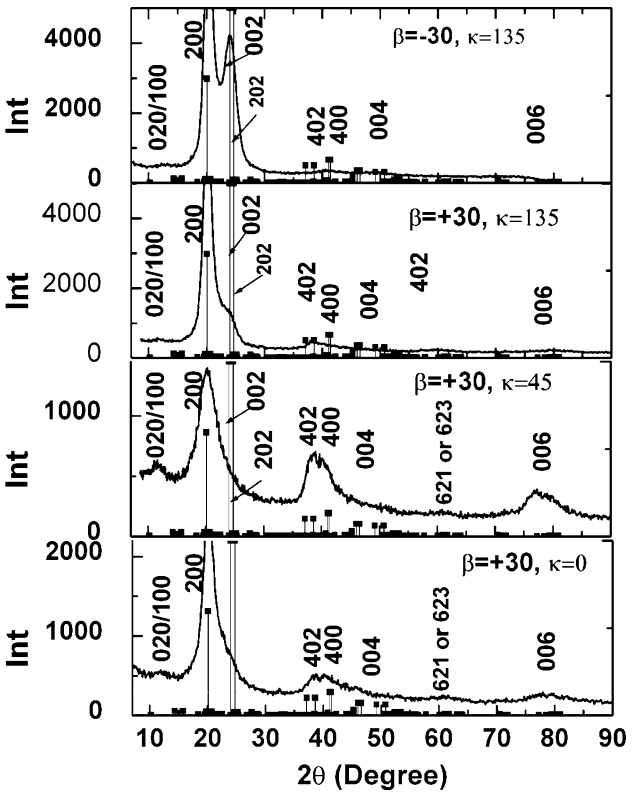

Fig. 16 Transmission intensity of XRD patterns for a biaxial drawn polyamide 6 film taken at its left side (L; see Fig. 2b). The film was oriented by the angles β and κ (see Fig. 14a)

References

1. Vasanthan N (2003) J Polym Sci: Part B: Polym Phys 41:2870
2. Beltrame P, Citterio C, Testa G, Seves A (1999) J Appl Polym Sci 74:1941
3. Arimoto H, Ishibashi M, Hirai M, Charani Y (1956) J Polym Sci: Part A 3:317
4. Stepaniak RF, Garton A, Carlsson DJ, Wiles DM (1979) J Appl Polym Sci 23:1747
5. Parker J, Lindenmeyer P (1977) J Appl Polym Sci 21:821
6. Holmes D, Bunn C, Smith J (1955) J Polym Sci 17:159
7. Huisman R, Heuvel H, Lind K (1976) J Polym Sci Polym Phys 14:921
8. Huisman R, Heuvel H (1976) J Polym Sci Polym Phys 14:941
9. Desper C, Stein R (1966) Journal of Applied Physics 37:3990
10. Decker B, Asp E, Harker D (1948) J Appl Phys 19:388
11. Riello P, Fagherazzi G, Canton P (1998) Acta Cryst A 54:219
12. Alexander L (1971) X-ray diffraction methods in polymer science. Wiley-Interscience, New York
13. Williamson G, Hall W (1953) Acta Metall 1:22
14. Dencheva N, Denchev Z, Oliveira M, Funari S (2007) J Appl Polym Sci 103:2242